Phytomedicine 23 (2016) 32–41

Contents lists available at ScienceDirect

Phytomedicine

journal homepage: www.elsevier.com/locate/phymed

Apoptosis and necroptosis induced by stenodactylin in neuroblastoma cells can be completely prevented through caspase inhibition plus catalase or necrostatin-1

Letizia Polito*, Massimo Bortolotti, Manuela Pedrazzi, Daniele Mercatelli, Maria Giulia Battelli, Andrea Bolognesi

Alma Mater Studiorum – University of Bologna, Department of Experimental, Diagnostic and Specialty Medicine-DIMES, General Pathology Unit, Via S. Giacomo 14, 40126 Bologna, Italy

ARTICLE INFO

Article history:
Received 4 August 2015
Revised 24 November 2015
Accepted 26 November 2015

Keywords:
Anti-cancer drug
Apoptosis
Neuroblastoma
Oxidative stress
Plant toxin
Ribosome-inactivating protein

ABSTRACT

Background: Stenodactylin is a highly toxic plant lectin purified from the caudex of *Adenia stenodactyla*, with molecular structure, intracellular routing and enzyme activity similar to those of ricin, a well-known type 2 ribosome-inactivating protein. However, in contrast with ricin, stenodactylin is retrogradely transported not only in peripheral nerves but also in the central nervous system.
Purpose: Stenodactylin properties make it a potential candidate for application in neurobiology and in experimental therapies against cancer. Thus, it is necessary to better clarify the toxic activity of this compound.
Study design: We investigated the mechanism of stenodactylin-induced cell death in the neuroblastoma-derived cell line, NB100, evaluating the implications of different death pathways and the involvement of oxidative stress.
Methods: Stenodactylin cytotoxicity was determined by evaluating protein synthesis and other viability parameters. Cell death pathways and oxidative stress were analysed through flow cytometry and microscopy. Inhibitors of apoptosis, oxidative stress and necroptosis were tested to evaluate their protective effect against stenodactylin cytotoxicity.
Results: Stenodactylin efficiently blocked protein synthesis and reduced the viability of neuroblastoma cells at an extremely low concentration and over a short time (1 pM, 24 h). Stenodactylin induced the strong and rapid activation of apoptosis and the production of free radicals. Here, for the first time, a complete and long lasting protection from the lethal effect induced by a toxic type 2 ribosome-inactivating protein has been obtained by combining the caspase inhibitor Z-VAD-fmk, to either the hydrogen peroxide scavenger catalase or the necroptotic inhibitor necrostatin-1.
Conclusion: In respect to stenodactylin cytotoxicity, our results: (i) confirm the high toxicity to nervous cells, (ii) indicate that multiple cell death pathways can be induced, (iii) show that apoptosis is the main death pathway, (iv) demonstrate the involvement of necroptosis and (v) oxidative stress.

Introduction

Stenodactylin is a highly toxic lectin purified from the caudex of *Adenia stenodactyla* (Pelosi et al. 2005; Stirpe et al. 2007) belonging to ribosome-inactivating proteins, a family of RNA *N*-glycosylases (EC 3.2.2.22) widely expressed throughout the plant kingdom (Di Maro et al. 2014). These plant toxins specifically cleave adenine from the highly conserved sarcin/ricin loop on eukaryotic 28S rRNA with different potencies. Some of these toxins also deadenylate other nucleotide substrates, such as mRNA, tRNA, DNA and poly(A); thus, it was proposed to classify them as polynucleotide:adenosine

Abbreviations: BHA, butylated hydroxyanisole; CAT, catalase; DAPI, 4′,6-diamidino-2-phenylindole; EC_{50} and ET_{50}, effective concentration and time required to reduce cell viability by 50%; ER, endoplasmic reticulum; IC_{50} and IT_{50}, concentration and time required to inhibit cell protein synthesis by 50%; $\Delta\psi m$, transmembrane electrical potential gradient; NAC, *N*-acetyl-L-cysteine; NaPyr, sodium pyruvate; Nec-1, necrostatin-1; PBS, phosphate buffered saline; PI, propidium iodide; ROS, reactive oxygen species; RPMI-1640, Roswell Park Memorial Institute medium 1640; SOD, superoxide dismutase; UPR, unfolded protein response; Z-VAD-fmk, carbobenzoxy-valyl-alanyl-aspartyl-[O-methyl]- fluoromethylketone.

* Corresponding author. Tel.: +39 051 2094700; fax: +39 051 2094746.
E-mail address: letizia.polito@unibo.it (L. Polito).

http://dx.doi.org/10.1016/j.phymed.2015.11.006

glycosylases (Barbieri et al. 2000; Bolognesi et al. 2002). Ribosome-inactivating proteins are structurally divided into two main groups: type 1 proteins comprise a single A-chain with enzymatic activity, and type 2 proteins comprise an A-chain linked to a lectin B-chain through a disulphide bond, the most well-known type 2 protein being ricin (Stirpe and Battelli 2006). The presence of the B-chain can facilitate the binding to the cell surface and mediate the entry of the whole toxin into the cell. Inside the cell, the A and B moieties are separated, and the active A-chain, freed from steric hindrance, exerts enzymatic activity. Although several type 2 ribosome-inactivating proteins are very toxic, a number of similar non-toxic proteins have been identified in some plant species (Battelli 2004), most of them belonging to the *Sambucus* genus (Ferreras et al. 2011). Stenodactylin shares the same intracellular routing observed for ricin; the high cytotoxicity of this compound has been associated with a high-affinity binding to receptors, great uptake and low proteolysis, thereby facilitating the re-uptake of non-degraded lectin (Battelli et al. 2010).

Although the mechanisms involved in the cytotoxicity of plant toxins are quite controversial, there are evidences that protein synthesis inhibition is not the main event (Das et al. 2012).

By damaging rRNA, ribosome-inactivating proteins are capable of activating the ribotoxic stress response with the following induction of mitogen-activated protein kinases (MAPKs) and programmed cell death. Moreover, these toxins have been suggested to induce the endoplasmic reticulum (ER) stress and the consequent unfolded protein response (UPR). This response is triggered by the accumulation of truncated and misfolded proteins in the ER lumen of intoxicated cells (Horrix et al. 2011). Using different cellular models, previous studies demonstrated that oxidative stress mediates cell death induced by several plant toxins, among which is abrin (Bora et al. 2010; Shih et al. 2001), *Viscum album* L. coloratum agglutinin (Kim et al. 2004), ricin (Sehgal et al. 2011) and trichosanthin (Zhang et al. 2001). It has also been suggested that saporin cytotoxicity could depend on direct DNA damage, because of: (i) the well-known deadenylating activity of ribosome-inactivating proteins on purified DNA (Barbieri et al. 1997; Battelli et al. 1997), (ii) the nuclear localisation of saporin and (iii) the contemporary presence of DNA gaps resulting from abasic sites in HeLa intoxicated cells (Bolognesi et al. 2012).

The ability of ribosome-inactivating proteins, either type 1 or type 2, to induce cell death through apoptosis has been extensively demonstrated using different *in vitro* and *in vivo* models (reviewed by Battelli 2004; Das et al. 2012). The exposure of cells to some plant toxins reduces the mitochondrial transmembrane electrical potential gradient ($\Delta\psi m$), resulting in the activation of caspases and subsequent apoptosis (Kim et al. 2004; Narayanan et al. 2004). The type 1 ribosome-inactivating protein saporin was reported to induce apoptotic cell death through mitochondrial cascade, independently of translation inhibition (Sikriwal et al. 2008). Beside the intrinsic pathway, also the extrinsic pathway of caspase activation has been demonstrated to be efficiently induced by type 2 ribosome-inactivating proteins (Polito et al. 2009).

In addition to apoptosis, increasing evidence suggests that these plant toxins elicit alternative molecular mechanisms that trigger different cell death programmes. Both caspase-dependent and independent cell death pathways have been described for several ribosome-inactivating proteins (Polito et al. 2009; Bora et al. 2010).

Following caspase inhibition, plant toxins kill cells through alternative cell death pathways that possess the morphological features of necrosis (Bora et al. 2010). Accumulating evidence has revealed that necrosis also functions as an alternative programmed mode of cell death, triggered through the same signals that induce apoptosis. This "programmed necrosis" has been defined as necroptosis, and this condition becomes evident when normal apoptosis has been blocked, for example, using caspase inhibitors. Necroptosis has been recently indicated as an independent pathway that can be particularly relevant in some cell types, including neurons (Degterev et al. 2005; You et al. 2008).

Plant toxins have received much attention concerning their application in medicine. After linking to appropriate carriers, particularly monoclonal antibodies (immunotoxins), these proteins have been used in experimental therapies against cancer, demonstrating particularly promising efficacy in haematological malignancies (Bolognesi and Polito 2004; Polito et al. 2011, 2013). Plant toxin-containing immunotoxins have also been used in neurobiology experiments (Wiley 2008).

All tested toxic lectins are retrogradely transported in peripheral nerves, whereas only *Adenia* toxins are also retrogradely transported in the central nervous system (Monti et al. 2007; Wiley and Kline 2000). This "suicide transport" facilitates the transport of toxins to the cell body for neuron killing. Thus, *Adenia* toxins could be used for targeted-lesioning experiments to induce the death of selected neuronal elements or populations.

Despite ribosome-inactivating proteins are known for a very long time, the exact mechanism of their toxicity remains unsolved and deserves to be clarified mainly because of their pharmacological use in medicine. Here, we investigated the mechanism of stenodactylin-induced cell death in a neuroblastoma-derived cell line, evaluating the implications of different death pathways and the involvement of oxidative stress.

Materials and methods

Reagents

Stenodactylin was purified from the caudex of *Adenia stenodactyla* as previously described (Stirpe et al. 2007). Purity was > 99%.

The pan-caspase inhibitor carbobenzoxy-valyl-alanyl-aspartyl-[O-methyl]- fluoromethylketone (Z-VAD-fmk, hereinafter indicated as Z-VAD) was purchased from Vinci-Biochem (Florence, Italy); necroptosis inhibitor necrostatin-1 (Nec-1), and the reactive oxygen species (ROS) scavengers, butylated hydroxyanisole (BHA), catalase (CAT), *N*-acetyl-L-cysteine (NAC), sodium pyruvate (NaPyr), superoxide dismutase (SOD) and (±)-6-hydroxy-2,5,7,8-tetramethylchromane-2-carboxylic acid (Trolox) were purchased from Sigma (Sigma-Aldrich, St. Louis, MO, USA). All other reagents were purchased from Sigma-Aldrich and were of analytical grade.

Cell culture

The human neuroblastoma-derived NB100 cell line (Bolognesi et al. 2013) was maintained at the logarithmic phase of growth in Roswell Park Memorial Institute medium 1640 (RPMI-1640), supplemented with 10% (v/v) heat-inactivated foetal bovine serum, 2 mM L-glutamine, 100 U/ml penicillin G and 100 μg/ml streptomycin (hereafter referred to as complete medium) at 37 °C in a humidified atmosphere containing 5% CO_2 in a HeraCell Haraeus incubator (Hanau, Germany).

Cell protein synthesis

NB100 cells (2×10^4/well) were seeded onto 24-well plates in 250 μl of complete medium in the absence (control cultures) or presence of stenodactylin. After 48 h, cell protein synthesis was evaluated as previously described (Battelli et al. 2010). The IC_{50} and IT_{50} (stenodactylin concentration and time required to inhibit cell protein synthesis by 50%) were calculated using linear regression analysis.

Cell viability

Cell viability was evaluated as previously described (Battelli et al. 2010). The EC_{50} and ET_{50} (stenodactylin effective concentration and time required to reduce cell viability by 50%) were calculated using

linear regression analysis. Stenodactylin toxicity was also evaluated using NB100 cells pretreated with 100 μM Z-VAD, 100 μM Nec-1, 30 μM BHA, 10 U/ml CAT, 30 μM NAC, 1 mM NaPyr, 100 U/ml SOD or 30 μM Trolox (the highest concentrations resulted not toxic for NB100 cells in preliminary tests). The reagents were added to cells 3 h before stenodactylin administration. The protective effect of Z-VAD, CAT and Nec-1 was also evaluated in two-by-two combination experiments, using the above reported concentrations and preincubation times. Subsequently, the cells were treated for 2 h with 10^{-12} M stenodactylin and, after washing with 5 mM sodium phosphate buffer, pH 7.5, containing 0.14 M NaCl (PBS), further incubated for the indicated times in complete medium.

Cell and nuclear morphology

The morphological analysis of the treated cells was conducted through phase contrast microscopy directly in 96-well plates using a digital camera from Motic Microscopes, (Xiamen, Fujian, China).

The nuclear morphology was captured after seeding NB100 cells (2×10^4/500 μl of complete medium) onto 10-mm coverslips in 24-well plates at 48 h prior to treatment. Subsequently, the cells were fixed with 2% *p*-formaldehyde for 30 min, washed with PBS, incubated with 7 μl DAPI (4′,6-diamidino-2-phenylindole)/antifade and visualized using a Nikon Eclipse E600W fluorescence microscope (Nikon, Melville, NY, USA).

Analysis of the mitochondrial transmembrane electrical potential gradient

The mitochondrial $\Delta\psi$m was examined after staining NB100 cells with the cationic, lipophilic dye JC-1 contained in the Mitochondria Staining Kit (Sigma-Aldrich), which upon aggregation, exhibits a fluorescence emission shift from 530 nm (green monomer) to 590 nm (red "J-aggregates"=healthy cells). The cells (2×10^4/500 μl) were directly seeded onto coverslips in 35-mm dishes at 48 h prior to treatment with stenodactylin for 24 h, and subsequently stained with 500 μl of JC-1 dye (1:100 in RPMI) and incubated at room temperature in the dark for 10 min. The cells were washed three times and observed under a fluorescence microscope.

AnnexinV/Propidium iodide (PI) analysis

Apoptotic and necrotic changes were detected through flow cytometry and fluorescence microscopy using the AnnexinV-EGFP Apoptosis Kit (BioVision, Inc., Milpitas, CA, USA).

Flow cytometry experiments: The cells (2×10^5/3 ml) were seeded in 25-cm^2 flasks and after 24 h treated with stenodactylin. After treatment, the cells were centrifuged at 400×g for 5 min, washed in 2 ml fresh medium, centrifuged again and stained according to the manufacturer's instructions. Within 30 min, the cells were analysed through flow cytometry on a FACSAria BD Analyser using FACSDiva software (Becton, Dickinson and Company, Franklin Lakes, NJ, USA).

Fluorescence microscopy experiments: The cells (1.5×10^4/500 μl) were directly seeded onto coverslips in 35-mm dishes at 48 h prior to the experiments. After the indicated time, 198 μl of binding buffer, 1 μl of AnnexinV-EGFP and 1 μl of PI were added. Following incubation at room temperature for 10 min in the dark, the coverslips were inverted onto slides, and apoptotic cells ($AnnexinV^+/PI^-$), necrotic cells ($AnnexinV^-/PI^+$) and late stage apoptotic cells ($AnnexinV^+/PI^+$) were observed under a fluorescence microscope, as described above. Merged images were obtained using Image J 1.42q software.

Caspase 3/7 activity

The caspase 3/7 activity was assessed using the luminescent Caspase-Glo® 3/7 assay (Promega Corporation, Madison, WI, USA). The cells (4×10^3/well) were seeded onto 96-well microtiter plates in 100 μl of complete medium. After 24 h, the cells were treated with 10^{-12} M stenodactylin for the indicated times. Caspase 3/7 activation was evaluated as already described (Bolognesi et al. 2013). For experiments using inhibitors or scavengers, stenodactylin was added at 3 h after treatment with the inhibitors and the cells were further incubated for 2 h. Fresh medium containing the scavengers and the inhibitors was changed every 24 h.

Assessment of oxidative stress

The generation of ROS was detected through flow cytometry and fluorescence microscopy using the Superoxide Detection Kit (Enzo Life Sciences, Farmingdale, NY, USA).

Flow cytometry experiments: The cells (4×10^5/3 ml) were seeded in 25-cm^2 flasks and treated with stenodactylin 10^{-12} M for 8 h. After trypsinization, the cells were washed, and the pellet was re-suspended in 500 μl of Superoxide Detection Mix, according to the manufacturer's instructions. Within 30 min, the cells were analysed through flow cytometry, in PE-channel, using the FACSAria BD Analyser.

Fluorescence microscopy experiments: The cells (1.5×10^4/500 μl) were seeded directly onto coverslips in 35-mm dishes 48 h prior to stenodactylin (10^{-12} M) treatment. After 8 h, the medium was removed and 600 μl of Superoxide Detection Mix was added. Following incubation at 37 °C for 1 h in the dark, the cells were observed under a fluorescence microscope, as described above.

Statistical analysis

Statistical analyses were conducted using XLSTAT-Pro software, version 6.1.9 (Addinsoft 2003). The results are presented as the means ± S.D. of three different experiments. The data were analysed using ANOVA/Bonferroni test. The Dunnett's test was used in addiction to ANOVA, when necessary.

Results

Stenodactylin is toxic to NB100 cells at a very low concentration

The toxicity of stenodactylin towards NB100 cells was determined by evaluating both protein synthesis inhibition and viability reduction to assess the correlation between translation impairment and cell viability (Fig. 1).

Dose-response curves, shown in Fig. 1A, demonstrated that protein synthesis and cell viability proceed in a parallel manner. After 48 h, stenodactylin strongly reduced both protein synthesis and viability, with an IC_{50} of 4×10^{-14} M and an EC_{50} of 2.5×10^{-14} M. Both protein synthesis and viability were completely inhibited at a concentration of 10^{-12} M, and this concentration was used for all further experiments. In time-course experiments, stenodactylin significantly reduced protein synthesis after 6 h ($p < 0.01$), and an almost total arrest was observed after 16 h. However, stenodactylin did not significantly affect cell viability until 12 h, after this time cell viability rapidly sloped and was completely abolished after 24 h (Fig. 1B).

Stenodactylin induces a strong and rapid activation of apoptosis

We examined the presence of cellular and nuclear morphological changes in NB100 cells treated for 24 h with stenodactylin using phase contrast microscopy and fluorescence microscopy, respectively. The visual inspection of stenodactylin treated NB100 cells with phase contrast microscopy showed morphological features characteristic of apoptosis, including cell shrinkage, cell membrane blebbing, and cytoplasmic condensation (Fig. 2A). Nuclear examination through fluorescence microscopy after DAPI staining showed the

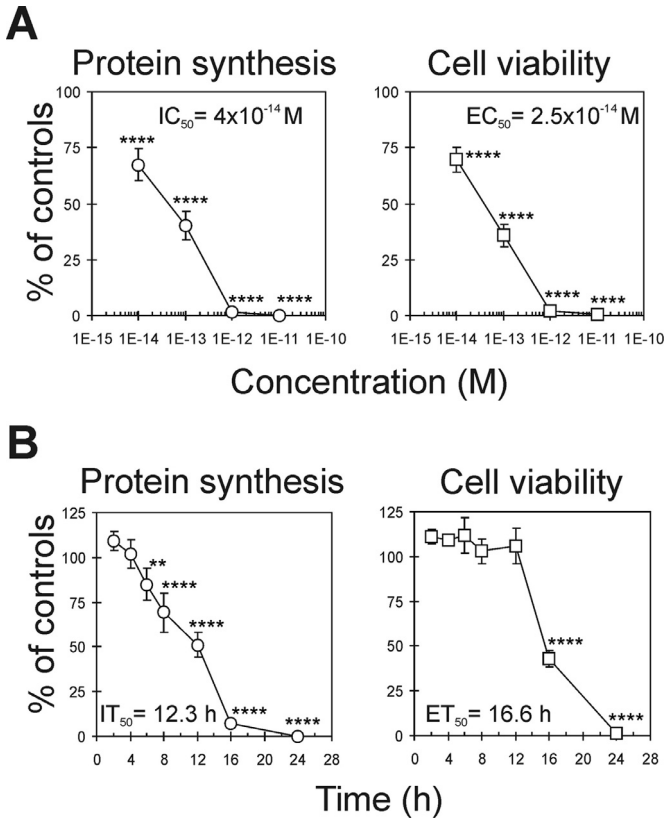

Fig. 1. Effect of stenodactylin on protein synthesis and viability in NB100 cells. Protein synthesis (○) and cell viability (□) were evaluated at 48 h after exposure to the indicated concentrations of stenodactylin (A) or in time-course experiments with cells exposed to 10^{-12} M stenodactylin (B). The mean results ± S.D. are reported, representing the percentage of control values obtained from cultures grown in the absence of stenodactylin. IC_{50} and IT_{50} are the concentration and the time required to inhibit 50% of protein synthesis. EC_{50} and ET_{50} are the concentration and the time required to reduce cell viability by 50%. Data were analysed by ANOVA/Bonferroni test, followed by a comparison with Dunnett's test (confidence range 95%; ** $p < 0.01$ *versus* untreated cells, **** $p \leq 0.0001$ *versus* untreated cells).

presence of chromatin condensation and nuclear blebs (Fig. 2B). Alterations of the $\Delta\psi$m were detected through fluorescence in cells exposed to stenodactylin for 24 h after staining with JC-1 (Fig. 2C). In control cells, JC-1 formed characteristic J-aggregates in mitochondria, yielding red fluorescence, whereas in stenodactylin-treated cells, JC-1 remained in the monomeric form, producing green fluorescence, indicating low $\Delta\psi$m. These results confirm that cells undergo apoptosis after stenodactylin intoxication and that mitochondria are involved.

Double staining with AnnexinV/PI through flow cytometry demonstrated that most NB100 cells treated with stenodactylin for 24 h showed the typical features of late stage apoptosis (Fig. 2D).

To demonstrate the involvement of caspase-dependent apoptosis, caspase 3/7 activation was measured in cells exposed to stenodactylin for different incubation times from 2 h to 16 h (Fig. 2E). This experiment showed the strong activation of effector caspases, which became significant after 4 h ($p < 0.05$) and with a plateau observed after 8 h and a 770% activation value compared with untreated cells.

Reactive oxygen species scavengers protect cells from stenodactylin toxicity

To verify the involvement of ROS after treatment with stenodactylin the level of superoxide anion was measured through both fluorescence microscopy and cytofluorometry. The presence of superoxide was demonstrated in NB100 cells treated with stenodactylin for

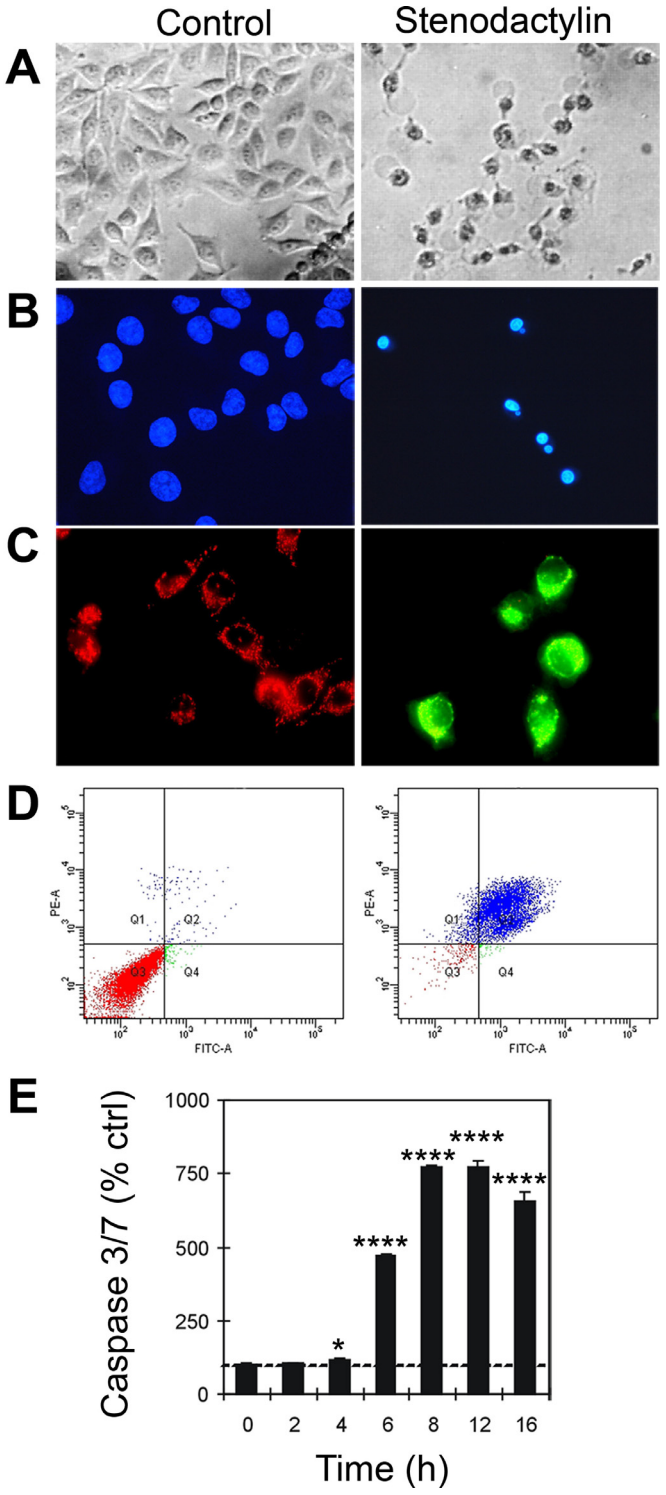

Fig. 2. Activation of apoptosis through stenodactylin in NB100 cells. Cells were cultured in the absence or in the presence of 10^{-12} M stenodactylin for 24 h. Morphology of cells was assessed using phase contrast microscopy (600×) (A) and fluorescence microscopy after incubation with DAPI (600×) (B). Mitochondrial transmembrane potential of cells was followed by staining with JC-1 and analysis through fluorescence microscopy (600×) (C). Apoptosis/necrosis was evaluated after AnnexinV/PI staining and flow cytometry analysis. Representative plots of AnnexinV (FITC channel)/PI (PE channel) staining of NB100 cells are shown (D). Caspase 3/7 activation was determined in cells treated with 10^{-12} M stenodactylin for different times (2–16 h). The mean results ± S.D. are reported, representing the percentage of control values obtained from cultures grown in the absence of stenodactylin. Data were analysed by ANOVA/Bonferroni test, followed by a comparison with Dunnett's test (confidence range 95%; * $p < 0.05$ *versus* untreated cells, **** $p \leq 0.0001$ *versus* untreated cells) (E).

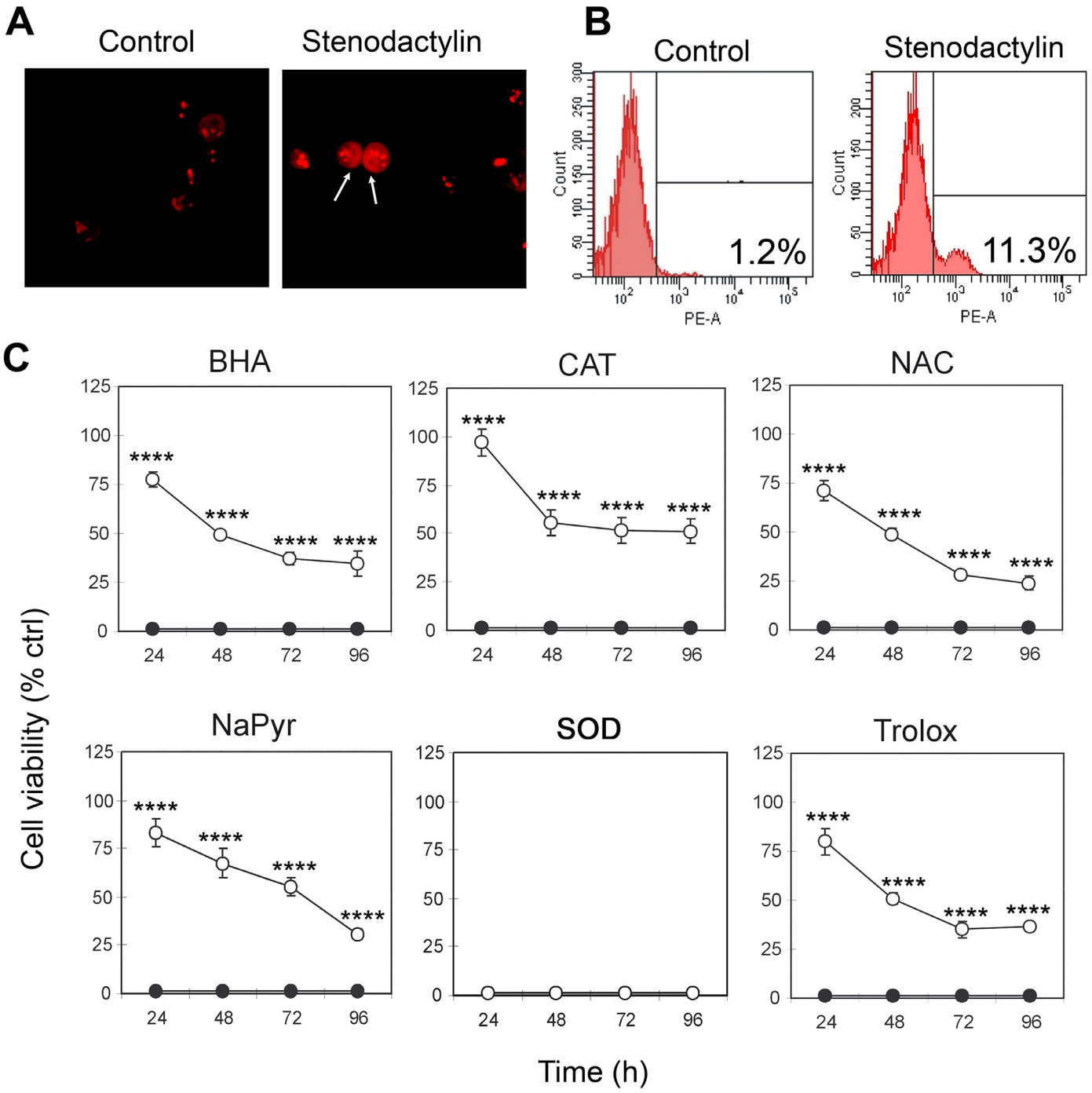

Fig. 3. Involvement of oxidative stress induced through stenodactylin in NB100 cells. Superoxide production in NB100 cells treated with stenodactylin (10^{-12} M) for 8 h was assessed using fluorescence microscopy (600×) (A) and cytofluorometry (B). Cells were treated for 2 h with stenodactylin alone (•) or preceded by a 3-h preincubation with the scavengers (30 μM BHA, 10 U/ml CAT, 30 μM NAC, 1 mM NaPyr, 100 U/ml SOD or 30 μM Trolox) (○), and viability was measured at the indicated times (C). The results are presented as the means ± S.D. of three independent experiments performed in triplicate, representing the percentage of control values obtained from cultures grown in the absence of the lectin. Data were analysed by ANOVA/Bonferroni test (confidence range 95%; **** $p \leq 0.0001$ *versus* cells treated with stenodactylin alone).

8 h through both fluorescence microscopy (Fig. 3A) and cytofluorometry (Fig. 3B), revealing that 11.3% of cells were positive to superoxide, in contrast with the 1.2% of positive cells reported for untreated cells.

To further analyse the contribution of ROS in cell death pathways induced by stenodactylin, the protective role of several ROS scavengers, *i.e.*, BHA, CAT, NAC, NaPyr, SOD and Trolox in stenodactylin-intoxicated cells was investigated in time-response experiments (24–96 h) (Fig. 3C). No protection from stenodactylin induced cell death was observed pretreating cells with SOD. All the other scavengers gave a strong cell protection. The protective effect was higher at 24 h (75–100% of cell survival) and decreased over time, though at 96 h 25–50% of cells are still alive. The highest level of protection was reported for CAT, leading to the survival of approximately 100% of treated cells after 24 h, and about 50% after 48 h, this effect was maintained at all the other tested times (up to 96 h).

To demonstrate that the protection exerted through CAT reflects the enzymatic activity of this molecule, the cells were pretreated with CAT previously inactivated with heat for 30 min at 65 °C. As expected, no protective effect towards stenodactylin was observed (data not shown).

Stenodactylin toxicity is considerably reduced through the inhibition of the apoptotic or necroptotic pathway

To determine the role of caspase-dependent programmed cell death, the pan-caspase inhibitor Z-VAD, which irreversibly binds to the catalytic site of caspases, was used to selectively inhibit the apoptotic pathway. NB100 cells were pretreated and maintained in 100 μM Z-VAD, and the cell viability was determined at different time points (24, 48, 72 and 96 h). As shown in Fig. 4A, Z-VAD completely blocked caspase activation at all the considered time points. Such caspase inhibition reduced almost to zero the cytotoxicity of stenodactylin after 24 h from intoxication. However, the protective effect of the pan-caspase inhibitor decreased over time, leading to 10% viability after 96 h. These results not only demonstrated the prevalence of apoptosis in the first 24 h but also indicated the involvement of caspase-independent cell death pathways. Moreover, in the presence of the necroptosis inhibitor Nec-1, stenodactylin-induced cell death was strongly reduced at 24 h, with a viability of approximately 70%. Subsequently at 48, 72 and 96 h, cell viability decreased to approximately 25%. Therefore, Nec-1 was slightly more effective than Z-VAD in protecting cells from long-term intoxication (Fig. 4B).

After 72–96 h, cells pretreated with Z-VAD appeared small, with round or oval shape and pyknotic nuclei. In contrast, cells pretreated with Nec-1 showed heterogeneous cellular and nuclear morphological characteristics, with the presence of both shrunken and rounded cells (Fig. 4C)

The cells were subjected to AnnexinV/PI double staining after treatment with stenodactylin in the presence or absence of the two inhibitors to confirm the death pathway(s) primarily involved after 48 h of treatment (Fig. 4D). Typical double fluorescence, compatible with late apoptosis, was observed in stenodactylin-intoxicated cells. However, only red fluorescence was observed in cells pretreated with Z-VAD, indicating the membrane damage and PI staining typical of non-apoptotic death. In contrast, double fluorescence was observed for cells pretreated with Nec-1.

Full rescue of NB100 cells from stenodactylin toxicity by combining Z-VAD to either catalase or necrostatin-1

The viability of NB100 cells pretreated with ROS scavengers in the absence or in the presence of Z-VAD, followed by stenodactylin treatment was measured after 72 h (Fig. 5A). All the tested scavengers were able to significantly protect neuroblastoma cells from stenodactylin intoxication. The scavengers CAT and NaPyr gave the higher cell protection (52 and 55%, respectively) with respect to NAC, Trolox and BHA (ranging from 29% to 38%). When ROS scavengers were co-administered with Z-VAD, their protective effect was in all cases significantly augmented ($p \leq 0.0001$). The co-administration of CAT and Z-VAD completely rescued NB100 cells from stenodactylin-induced cell death after 72 h (Fig. 5A).

To determine the relationship between ROS blockage and caspase activation in stenodactylin-treated cells, AnnexinV positivity and caspase 3/7 activation were evaluated in cells pretreated with CAT. After 72 h, double staining with AnnexinV/PI showed the typical pattern of early and late apoptosis in stenodactylin-treated cells (Fig. 5B). Time-course experiments (24–96 h) demonstrated that caspases are activated after 24 h of incubation with stenodactylin, with a plateau observed starting from 48 h, showing approximately 300% activation compared with control and 50% cell viability (Fig. 5C). The maximal value of caspase 3/7 activation through stenodactylin in the presence of CAT was significantly lower ($p \leq 0.0001$) than that obtained in absence of the scavenger (compare Fig. 2E and Fig. 5C). These results confirmed that the apoptotic pathway is also activated in cells pretreated with CAT, although after longer times and to a lesser extent.

Cell viability was also evaluated in time-course experiments after combined pretreatment, Z-VAD + CAT, Z-VAD + Nec-1 or CAT + Nec-1. The combination CAT + Nec-1 did not ensure a long-term protection of NB100 cells. However, the combination of the pan-caspase inhibitor and the hydrogen peroxide scavenger and the combination of the pan-caspase inhibitor and the necroptosis inhibitor completely inhibited stenodactylin-induced cell death at all times, even at 96 h (Fig. 5D).

Discussion

Stenodactylin is one of the most cytotoxic type 2 plant toxins, particularly towards nervous cells (Monti et al. 2007). Accordingly, in the present study, stenodactylin completely abolished neuroblastoma protein synthesis and cell viability at an extremely low concentration and in a short time (1 pM, 24 h), making this toxin an attractive candidate for the design and production of drugs for clinical application (Wiley and Lappi 2001; Bolognesi and Polito 2004).

Understanding the cell death pathways elicited through a potential drug represents a milestone in preclinical studies. Considering the results obtained at 24 h, all the evidences seemed to indicate the apoptosis as the principal/exclusive mechanism responsible of NB100 death by stenodactylin: cellular and nuclear morphology compatible with an apoptotic pattern, elevated AnnexinV positivity, altered mitochondrial transmembrane potential, and strong and rapid caspase activation. Furthermore, during the same time period, the pan-caspase inhibitor Z-VAD almost completely rescued the cells from death after stenodactylin exposure, demonstrating that the apoptotic pathway is the dominant and fastest death mechanism induced through stenodactylin. However, the lack of total protection at incubation periods longer than 24 h indicates that the toxin activates other cell death mechanisms.

Oxidative stress has already been shown to significantly contribute to plant toxin cytotoxicity. A mutant form of abrin, lacking *N*-glycosylase activity, induced apoptosis through an increase in intracellular ROS levels (Shih et al. 2001). The depletion of cellular antioxidants or increased ROS production induced apoptosis through mitochondria-dependent and mitochondria-independent pathways (Sinha et al. 2013). Treatment with antioxidant compounds conferred significant protection in Jurkat cells through the restoration of the antioxidant enzymes depleted after abrin treatment (Saxena et al. 2014).

Our results show that stenodactylin induces the early formation of superoxide anion that is almost coincident with the caspase activation, thus suggesting that ROS molecules can be important mediators of stenodactylin-induced apoptosis.

To assess the ROS involvement in stenodactylin intoxication of neuroblastoma cells we investigated the effect of scavengers and antioxidant compounds. Indeed, after 24 h, BHA, CAT, NAC, NaPyr and Trolox showed strong protective effects, sparing the cells from the intoxication consequences and allowing the survival of 75–100% of cell population. No protection was conferred after the addition of SOD, possibly reflecting the fact that in our experimental conditions the enzyme cannot easily reach the intracellular compartment where the superoxide is produced. The protective effect of scavengers decreased over the time. CAT was the most efficient antioxidant, with 50% of cells remaining viable after incubation for 96 h. In CAT pretreated cells caspase activation was delayed and reached levels of about half compared to not pretreated cells, indicating a correlation between hydrogen peroxide production and apoptosis.

Oxidative stress plays a significant pathogenic role in neuron death, indicating that endogenous antioxidant resources are inadequate or easily overwhelmed in neuronal cells (Uttara et al. 2009). The generation of ROS may be dependent on UPR resulting from increased protein folding load in ER (reviewed by Farooqi et al. 2015). UPR can protect the cell by increasing the transcription of ER chaperones; although persistent ER stress can lead to apoptotic cell death.

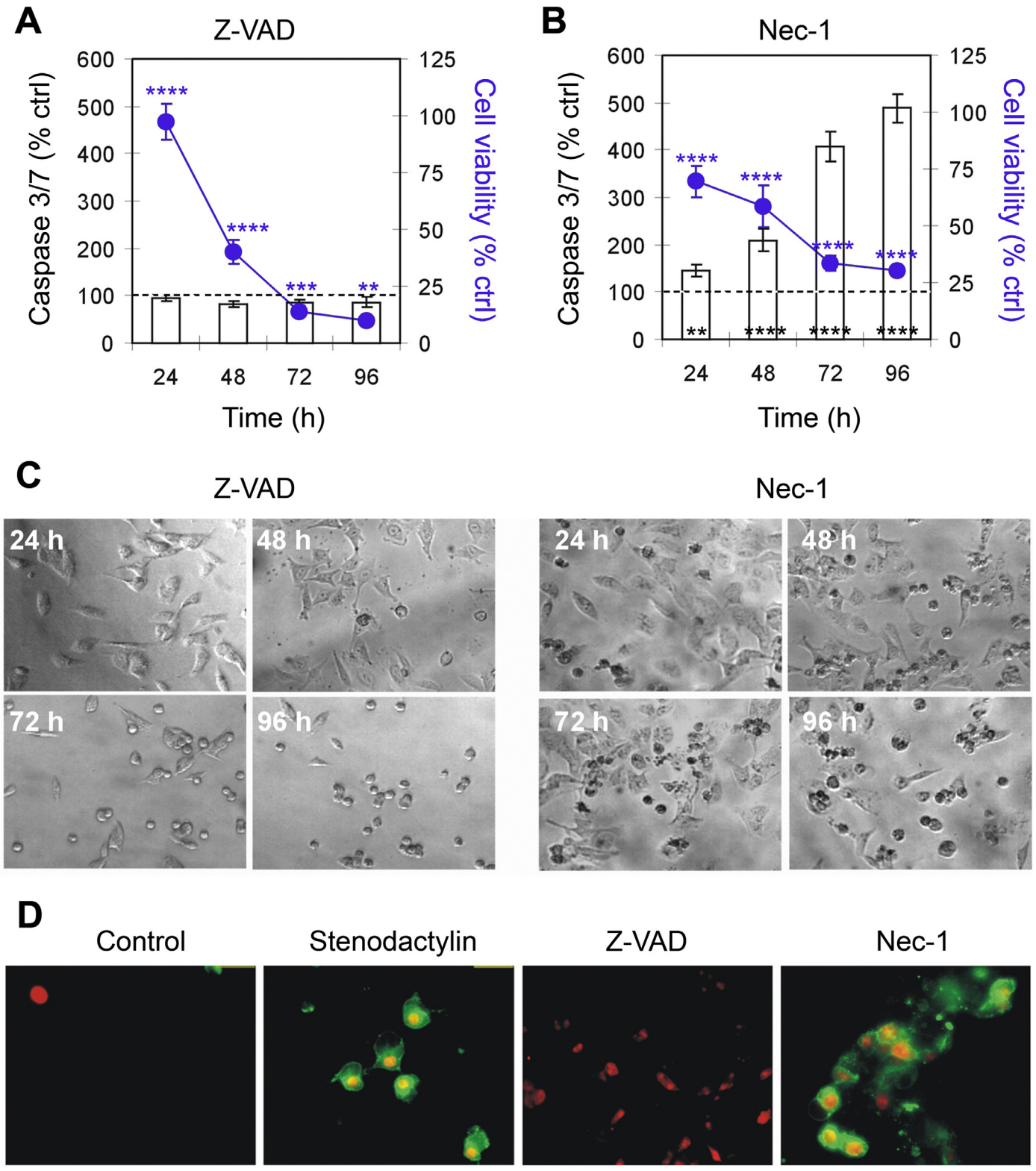

Fig. 4. Protective effects of the inhibitors Z-VAD (apoptosis) and Nec-1 (necroptosis) in NB100 cells treated with stenodactylin. The cells were pretreated for 3 h with Z-VAD (A) or Nec-1 (B) (100 μM), followed by treatment with 10^{-12} M stenodactylin for 2 h. Viability (•) and caspase 3/7 activity (columns), expressed as the percentage of control values obtained from cultures grown in the absence of stenodactylin, were evaluated at the indicated times. The results are presented as the means ± S.D. of three independent experiments performed in triplicate. Data were analysed by ANOVA/Bonferroni test, followed by a comparison with Dunnett's test for caspase experiments (confidence range 95%; ** $p < 0.01$, *** $p < 0.001$, **** $p \leq 0.0001$ *versus* cells treated with stenodactylin alone, in the case of cell viability, or *versus* untreated cells, in the case of caspase 3/7 activation). The morphology of cells treated with stenodactylin in the presence of the inhibitors was analysed using phase contrast microscopy (600×) (C) and double staining with AnnexinV (green)/PI (red), followed by fluorescence microscopy at 48 h after treatment (600×) (D).

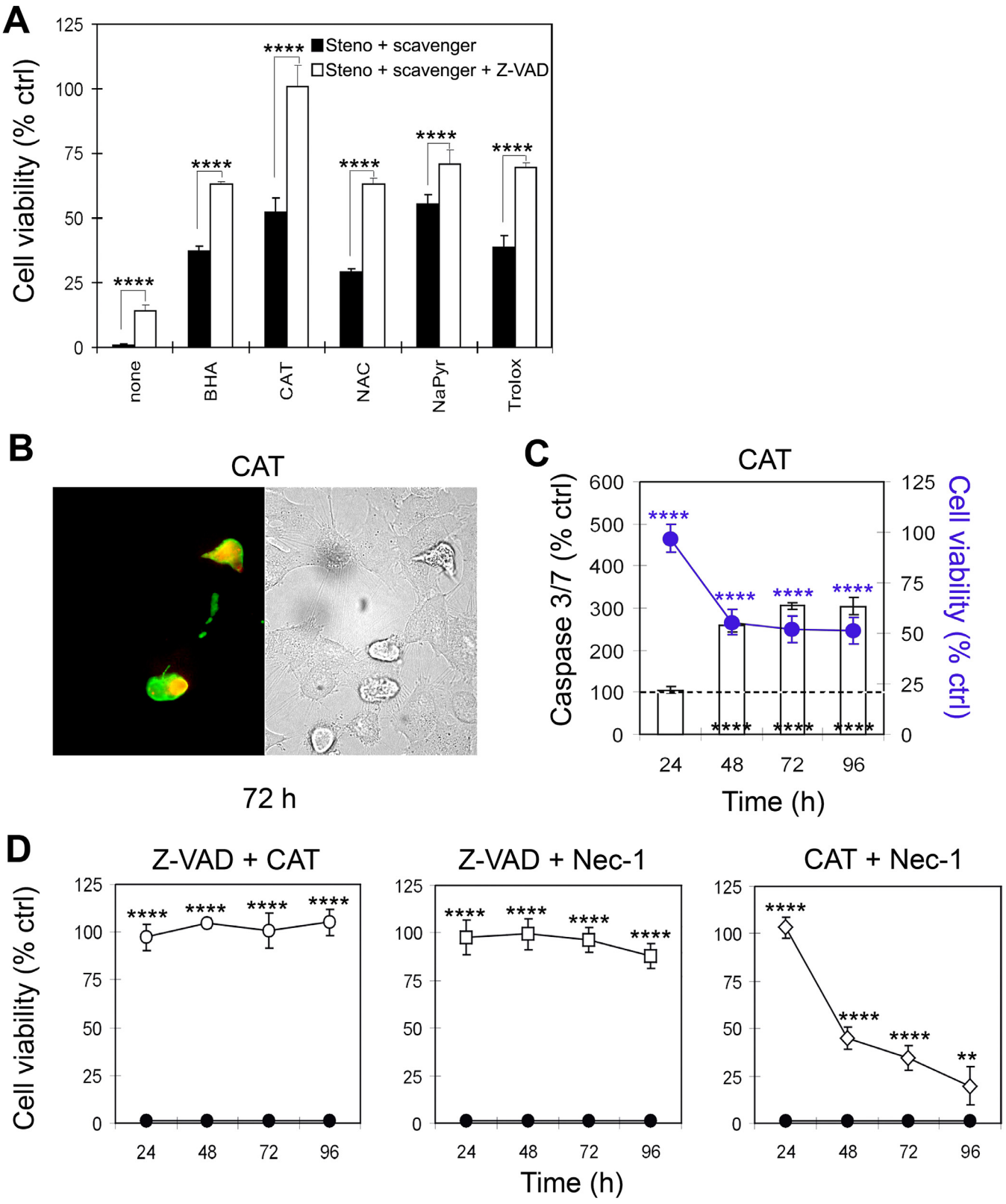

Fig. 5. Protection obtained through combinations of inhibitors and scavengers. NB100 cells were incubated for 2 h with 10^{-12} M stenodactylin alone or preceded by a 3-h preincubation with the scavengers (30 μM BHA, 10 U/ml CAT, 30 μM NAC, 1 mM NaPyr or 30 μM Trolox) (black columns) or with the scavengers + 100 μM Z-VAD (white columns). The viability was measured after 72 h. The statistical analysis was performed using ANOVA/Bonferroni (confidence range 95%; **** $p \leq 0.0001$ *versus* cells treated with stenodactylin with the scavenger and without Z-VAD) (A). NB100 cells were incubated with stenodactylin after pretreatment with CAT as above. Apoptosis and necrosis were evaluated through AnnexinV/PI double staining after 72 h using fluorescence microscopy (left) or light microscopy (right) (600×) (B). Caspase 3/7 activation (columns) and cell viability (●) induced through stenodactylin after pretreatment with CAT, were evaluated at different times (24–96 h) (C). The viability of cells treated with stenodactylin alone (●) or after preincubation with Z-VAD + CAT, (○), Z-VAD + Nec-1 (100 μM) (□) or CAT + Nec-1 (◊) was reported (D). Cell viability and caspase activation results are presented as the means ± S.D. of three independent experiments performed in triplicate. Data were analysed by ANOVA/Bonferroni test, followed by a comparison with Dunnett's test for caspase experiments (confidence range 95%; ** $p < 0.01$, **** $p \leq 0.0001$ *versus* cells treated with stenodactylin alone, in the case of cell viability, or *versus* untreated cells, in the case of caspase 3/7 activation).

ER is connected to mitochondria via the mitochondria-associated ER membranes, which regulate calcium homeostasis, mitochondrial function, autophagy and apoptosis and are implicated in neurodegenerative diseases (reviewed by Vance 2014).

Previous studies have implicated roles for ROS molecules also as initiators, modulators or effectors of necroptosis (reviewed by Vandenabeele et al. 2010). Necroptosis is initiated through tumour necrosis factor receptor activation and depends on the serine-threonine kinase receptor-interacting proteins 1 (RIPK1) and 3 (RIPK3) and other proteins. Nec-1 blocks necroptosis through the inhibition of RIPK1 activity (Degterev et al. 2005; Vandenabeele et al. 2010). Pretreatment of NB100 cells with Nec-1 prior to stenodactylin incubation preserved approximately 70% of cells after 24 h. The caspase activation was slower and lower in the presence of Nec-1, demonstrating that the necroptosis blockage can also delay the apoptotic pathway and suggesting that apoptosis and necroptosis share some molecular mechanisms during the first phase of the two processes. When NB100 cells were pretreated with the necroptosis inhibitor Nec-1, approximately 25% of stenodactylin-intoxicated cells remained viable after 96 h, suggesting that at this time, necroptosis is responsible for the death in approximately one-fourth of the cell population.

In the present study, after 24 h, death inhibitors and ROS scavengers were significantly efficient in protecting neuroblastoma cells from stenodactylin cytotoxicity. However, after longer incubation times, this protection considerably decreased. Thus, we conducted additional experiments treating cells with two-by-two combinations of Z-VAD, Nec-1 and CAT. The simultaneous administration of Z-VAD + Nec-1 completely abolished stenodactylin-induced cell death. The total long-term protection of neuroblastoma cells was also observed after preincubating the cells with Z-VAD + CAT, but not with Nec-1 + CAT. These results suggested the complementary action of apoptosis and necroptosis in neuroblastoma cells and the more rapid activation of apoptosis compared with necroptosis.

The caspase-dependent pathway and ROS production were the main cell death mechanisms involved in NB100 cell toxicity through stenodactylin. However, it is not clear whether ROS production is apoptosis dependent or whether these molecules are responsible for apoptosis induction. There are controversial reports on the role of caspase 3 in the formation of ROS; indeed, caspase 3 has been implicated in the production of reactive species, while in other cases, hydrogen peroxide has been reported to activate the caspase cascade (Zhang et al. 2001). In the present study, hydrogen peroxide production was more strongly associated with necroptosis. In the presence of Z-VAD, the protection conferred through CAT largely overlapped with that conferred through Nec-1, suggesting that necroptosis is related to ROS production, at least in nervous cells.

The idea that stenodactylin elicits more than one cell death pathway and the identification of mechanisms involved in stenodactylin-induced cell killing would provide useful insights for the potential application of stenodactylin in neurobiology and medicine. Indeed, the contribution of necroptosis has been implicated in neurological disorder, but few *in vitro* and animal models are available. The characteristic of retrograde transport in peripheral nerves and in the central nervous system and the ability of stenodactylin to kill neurons through apoptosis and necroptosis could be exploited to develop a molecular tool for new experimental models of neurodegenerative diseases.

In conclusions, our results confirm that the high stenodactylin toxicity to nervous cells depends on multiple cell death pathways, which involve mainly apoptosis, but also necroptosis and the production of free radicals. Moreover, here for the first time, a complete and long lasting protection from the lethal effect induced by a toxic type 2 ribosome-inactivating protein has been obtained by combining the caspase inhibitor Z-VAD, to either the hydrogen peroxide scavenger catalase or the necroptotic inhibitor necrostatin-1.

Conflict of interest

We wish to confirm that there are no known conflicts of interest associated with this publication and there has been no significant financial support for this work that could have influenced its outcome.

Acknowledgements

This work was supported by funds for selected research topics from the Alma Mater Studiorum – University of Bologna and by the Pallotti Legacies for Cancer Research.

References

Barbieri, L., Bolognesi, A., Valbonesi, P., Polito, L., Olivieri, F., Stirpe, F., 2000. Polynucleotide: adenosine glycosidase activity of immunotoxins containing ribosome-inactivating proteins. J. Drug Target. 8, 281–288.

Barbieri, L., Valbonesi, P., Bonora, E., Gorini, P., Bolognesi, A., Stirpe, F., 1997. Polynucleotide:adenosine glycosidase activity of ribosome-inactivating proteins: effect on DNA, RNA and poly(A). Nucleic Acids Res 25, 518–522.

Battelli, M.G., 2004. Cytotoxicity and toxicity to animals and humans of ribosome-inactivating proteins. Mini Rev. Med. Chem. 4, 513–521.

Battelli, M.G., Barbieri, L., Bolognesi, A., Buonamici, L., Valbonesi, P., Polito, L., Van Damme, E.J., Peumans, W.J., Stirpe, F., 1997. Ribosome-inactivating lectins with polynucleotide:adenosine glycosidase activity. FEBS Lett 408, 355–359.

Battelli, M.G., Scicchitano, V., Polito, L., Farini, V., Barbieri, L., Bolognesi, A., 2010. Binding and intracellular routing of the plant-toxic lectins, lanceolin and stenodactylin. Biochim. Biophys. Acta 1800, 1276–1282.

Bolognesi, A., Chatgilialoglu, A., Polito, L., Ferreri, C., 2013. Membrane lipidome reorganization correlates with the fate of neuroblastoma cells supplemented with fatty acids. PLoS One 8, e55537.

Bolognesi, A., Polito, L., 2004. Immunotoxins and other conjugates: pre-clinical studies. Mini Rev. Med. Chem. 4, 563–583.

Bolognesi, A., Polito, L., Lubelli, C., Barbieri, L., Parente, A., Stirpe, F., 2002. Ribosome-inactivating and adenine polynucleotide glycosylase activities in *Mirabilis jalapa* L. tissues. J. Biol. Chem. 277, 13709–13716.

Bolognesi, A., Polito, L., Scicchitano, V., Orrico, C., Pasquinelli, G., Musini, S., Santi, S., Riccio, M., Bortolotti, M., Battelli, M.G., 2012. Endocytosis and intracellular localisation of type 1 ribosome-inactivating protein saporin-s6. J. Biol. Regul. Homeost. Agents. 26, 97–109.

Bora, N., Gadadhar, S., Karande, A.A., 2010. Signaling different pathways of cell death: Abrin induced programmed necrosis in U266B1 cells. Int. J. Biochem. Cell. Biol. 42, 1993–2003.

Das, M.K., Sharma, R.S., Mishra, V., 2012. Induction of apoptosis by ribosome inactivating proteins: importance of N-glycosidase activity. Appl. Biochem. Biotechnol. 166, 1552–1561.

Degterev, A., Huang, Z., Boyce, M., Li, Y., Jagtap, P., Mizushima, N., Cuny, G.D., Mitchison, T.J., Moskowitz, M.A., Yuan, J., 2005. Chemical inhibitor of nonapoptotic cell death with therapeutic potential for ischemic brain injury. Nat. Chem. Biol. 1, 112–119.

Di Maro, A., Citores, L., Russo, R., Iglesias, R., Ferreras, J.M., 2014. Sequence comparison and phylogenetic analysis by the Maximum Likelihood method of ribosome-inactivating proteins from angiosperms. Plant Mol. Biol. 85, 575–588.

Farooqi, A.A., Li, K.T., Fayyaz, S., Chang, Y.T., Ismail, M., Liaw, C.C., Yuan, S.S., Tang, J.Y., Chang, H.W., 2015. Anticancer drugs for the modulation of endoplasmic reticulum stress and oxidative stress. Tumour Biol 36, 5743–5752.

Ferreras, J.M., Citores, L., Iglesias, R., Jiménez, P., Girbés, T., 2011. Use of ribosome-inactivating proteins from *Sambucus* for the construction of immunotoxins and conjugates for cancer therapy. Toxins 3, 420–441.

Horrix, C., Raviv, Z., Flescher, E., Voss, C., Berger, M.R., 2011. Plant ribosome-inactivating proteins type II induce the unfolded protein response in human cancer cells. Cell. Mol. Life Sci. 68, 1269–1281.

Kim, W.H., Park, W.B., Gao, B., Jung, M.H., 2004. Critical role of reactive oxygen species and mitochondrial membrane potential in Korean mistletoe lectin-induced apoptosis in human hepatocarcinoma cells. Mol. Pharmacol. 66, 1383–1396.

Monti, B., D'Alessandro, C., Farini, V., Bolognesi, A., Polazzi, E., Contestabile, A., Stirpe, F., Battelli, M.G., 2007. *In vitro* and *in vivo* toxicity of type 2 ribosome-inactivating proteins lanceolin and stenodactylin on glial and neuronal cells. Neurotoxicology 28, 637–644.

Narayanan, S., Surolia, A., Karande, A.A., 2004. Ribosome-inactivating protein and apoptosis: abrin causes cell death via mitochondrial pathway in Jurkat cells. Biochem. J. 377, 233–240.

Pelosi, E., Lubelli, C., Polito, L., Barbieri, L., Bolognesi, A., Stirpe, F., 2005. Ribosome-inactivating proteins and other lectins from Adenia (Passifloraceae). Toxicon 46, 658–663.

Polito, L., Bortolotti, M., Farini, V., Battelli, M.G., Barbieri, L., Bolognesi, A., 2009. Saporin induces multiple death pathways in lymphoma cells with different intensity and timing as compared to ricin. Int. J. Biochem. Cell Biol. 41, 1055–1061.

Polito, L., Bortolotti, M., Mercatelli, D., Battelli, M.G., Bolognesi, A., 2013. Saporin-S6: a useful tool in cancer therapy. Toxins 5, 1698–1722.

Polito, L., Bortolotti, M., Pedrazzi, M., Bolognesi, A., 2011. Immunotoxins and other conjugates containing saporin-S6 for cancer therapy. Toxins 3, 697–720.

Saxena, N., Rao, P.V.L., Bhaskar, A.S., Bhutia, Y.D., 2014. Protective effects of certain pharmaceutical compounds against abrin induced cell death in Jurkat cell line. Int. Immunopharmacol. 21, 412–425.
Sehgal, P., Kumar, O., Kameswararao, M., Ravindran, J., Khan, M., Sharma, S., Vijayaraghavan, R., Prasad, G.B., 2011. Differential toxicity profile of ricin isoforms correlates with their glycosylation levels. Toxicology 282, 56–67.
Shih, S.F., Wu, Y.H., Hung, C.H., Yang, H.Y., Lin, J.Y., 2001. Abrin triggers cell death by inactivating a thiol-specific antioxidant protein. J. Biol. Chem. 276, 21870–21877.
Sikriwal, D., Ghosh, P., Batra, J.K., 2008. Ribosome inactivating protein saporin induces apoptosis through mitochondrial cascade, independent of translation inhibition. Int. J. Biochem. Cell Biol. 40, 2880–2888.
Sinha, K., Das, J., Pal, P.B., Sil, P.C., 2013. Oxidative stress: the mitochondria-dependent and mitochondria-independent pathways of apoptosis. Arch. Toxicol. 87, 1157–1180.
Stirpe, F., Battelli, M.G., 2006. Ribosome-inactivating proteins: progress and problems. Cell. Mol. Life Sci. 63, 1850–1866.
Stirpe, F., Bolognesi, A., Bortolotti, M., Farini, V., Lubelli, C., Pelosi, E., Chambery, A., Polito, L., Dozza, P., Strocchi, P., Parente, A., Barbieri, L., 2007. Characterization of highly toxic type 2 ribosome-inactivating proteins from *Adenia lanceolata* and *Adenia stenodactyla* (Passifloraceae). Toxicon 50, 94–105.
Uttara, B., Singh, A.V., Zamboni, P., Mahajan, R.T., 2009. Oxidative stress and neurodegenerative diseases: a review of upstream and downstream antioxidant therapeutic options. Curr. Neuropharmacol. 7, 65–74.
Vance, J.E., 2014. MAM (mitochondria-associated membranes) in mammalian cells: lipids and beyond. Biochim. Biophys. Acta. 1841, 595–609.
Vandenabeele, P., Galluzzi, L., Vanden Berghe, T., Kroemer, G., 2010. Molecular mechanisms of necroptosis: an ordered cellular explosion. Nat. Rev. Mol. Cell. Biol. 11, 700–714.
Wiley, R.G., 2008. Substance P receptor-expressing dorsal horn neurons: Lessons from the targeted cytotoxin, substance P-saporin. Pain 136, 7–10.
Wiley, R.G., Kline, R.H.IV., 2000. Neuronal lesioning with axonally transported toxins. J. Neurosci. Methods 103, 73–82.
Wiley, R.G., Lappi, D.A., 2001. Targeted toxins.. Curr. Protoc. Neurosci. Chapter 1:Unit1.7.
You, Z., Savitz, S.I., Yang, J., Degterev, A., Yuan, J., Cuny, G.D., Moskowitz, M.A., Whalen, M.J., 2008. Necrostatin-1 reduces histopathology and improves functional outcome after controlled cortical impact in mice. J. Cereb. Blood Flow Metab. 28, 1564–1573.
Zhang, C., Gong, Y., Ma, H., An, C., Chen, D., Chen, Z.L., 2001. Reactive oxygen species involved in trichosanthin-induced apoptosis of human choriocarcinoma cells. Biochem. J. 355, 653–661 Erratum in: 2001. Biochem. J. 358, 792.